SI Appendix

Soy et al. *PNAS* 2016

Molecular convergence of clock and photosensory pathways through PIF3-TOC1 interaction and co-occupancy of target promoters

Judit Soy, Pablo Leivar, Nahuel González-Schain, Guiomar Martín, Céline Diaz, Maria Sentandreu, Bassem Al-Sady, Peter H. Quail, and Elena Monte

SI Expanded Results

RESULTS SECTION: PIF3 and TOC1 display coincident co-binding to dawn-phased genes under diurnal short-day conditions.

CONTEXT: "Genome-wide reanalysis of ChIP sequencing (ChIP-seq) data for PIF-associated (5) and TOC1-associated (14) loci, using identical criteria for defining both (see *SI Appendix*, *SI Expanded Results* for details), revealed an overlap of 144 shared genes, representing 48% and 7% of the redefined TOC1- and PIF-bound loci (the PIF-TOC1 gene set), respectively (Fig. 1A)." (Quoted from Main-text Results).

Comparative analysis of PIF and TOC1 ChIP-seq targets

The original published peak-to-gene associations in the PIF and TOC1 ChIP-Seq analyses were established using separate criteria. For PIFs, 5,892 putative binding sites were defined as those with an associated peak within 5 kb upstream of the transcriptional start site (TSS) and with no intervening gene (1). For TOC1, 868 peak-to-gene associations were defined as those including binding peaks within 2 kb upstream of the 5'-end and 1 kb downstream of the 3'-end of the annotated gene (2). To be able to directly compare these lists of putative targets here, we filtered them by removing those peak-to-gene associations established with non-overlapping cutoff criteria. For the PIF putative targets, we eliminated those with peaks within 2-5 kb of the TSS. For the TOC1 peak-to-gene associations, we first removed those with binding peaks downstream and inside of the corresponding annotated gene, and next we eliminated the ones that contained an intervening gene within the 2 kb upstream of the 5'-end of the annotated

gene. By applying these filters, we generated a list of 4,272 peak-to-gene associations for PIFs corresponding to 2,247 non-redundant putative target genes with 3,457 associated peaks, and a list of 309 peak-to-gene associations for TOC1 corresponding to 303 non-redundant putative target genes with 249 associated peaks.

Comparison of the 2,247 and 303 unique PIF- and TOC1-bound genes, respectively, showed an overlap of 144 putatively co-bound targets (Fig 1.A) (Dataset S1). Using the gene phase analysis tool PHASER, we identified a subset of 49 of these genes with a peak phase of expression in SD at pre-dawn (phases 18-23), where phases 18 and 23 were significantly enriched (pvalue<0.05, and count/expected gene ratio>1.5) (Fig. 1B, Dataset S1), that we named "dawn-specific PIF-TOC1". Of the remaining genes, 75 (72 phased between 0-17 and 3 non-rhythmic) were considered "No dawn-specific PIF-TOC1" (Fig. 1B), and 20 had no data available (Dataset S1). The SD phase pattern of the 144 PIF and TOC1 co-targets was clearly distinct from the phase pattern of the "TOC1 only" subset (159 genes) that showed significant enrichment at phases 19 and 3, or of the "PIF-only" subset (2,103 genes) that did not show any significantly enriched phase (Fig. 1B) (Dataset S1), suggesting that co-binding by PIFs and TOC1 underlies the pre-dawn phase specificity of the "dawn-specific PIF-TOC1" under SD. In LD, the phase pattern of the three gene sets was different compared to SD: the 144 PIF and TOC1 co-bound genes showed significant enrichment at phases 23, 2, 3, 7, and 14 (SI Appendix, Fig. S1) (Dataset S1), whereas the "TOC1-only" showed significant enrichment at phases 22, 1, 3, 5, and 22, and the "PIF-only" subset at phases 19, 22, 23, 0, 1, 4, 5, and 8 (SI Appendix, Fig. S1) (Dataset S1). These observations are in agreement with previous data showing that the peak phase of expression depends on the external photoperiod (3).

A selection of previously defined PIF-target genes with a pre-dawn peak phase of expression in SD were also considered for further analysis, as it was predicted that they might correspond to putative TOC1 target genes not identified by Huang et al. (2012) (2): *PIL1* (*AT2G46970*), *PAR1* (*AT2G42870*), *IAA19* (*AT3G15540*), *YUCCA8* (*AT4G28720*), *IAA29* (*AT4G32280*), and *ATHB2* (*AT4G16780*) (Dataset S1). Indeed, binding of both PIF3 and TOC1 to some of these putative co-bound targets (*PIL1* and *PAR1*) was validated in independent ChIP assays in short day-grown seedlings expressing YFP-PIF3

and TOC1-GFP under their respective promoters, along with other "dawn-specific PIF-TOC1" genes (Fig. 1C). This was especially remarkable, as PIF and TOC1 ChIP-seq analyses were done using seedlings grown in different light regimes such as continuous darkness and shade conditions (1), or under 12/12 LD photocycles (2), respectively. Gene expression regulation by TOC1 and PIFs was also confirmed for all these selected genes under SD conditions (Fig. 3 and 4, and SI Appendix, Fig. S5).

CONTEXT: "ChIP-quantitative PCR assays confirmed the direct binding of TOC1 and PIF3 to the promoters of selected predawn-specific PIF-TOC1 genes at postdusk [zeitgeber time (ZT)14] and dawn (ZT24), respectively (Fig. 1C), when each protein is most abundant in the SD diurnal cycle, respectively (*SI Appendix*, Fig. S2A and B and see *SI Appendix, SI Expanded Results* for details) (5, 14)." (Quoted from Main-text Results).

Temporal binding patterns of TOC1 and PIF3 to direct-target genes

Direct binding of PIF and TOC1 to a selection of "pre-dawn-specific PIF-TOC1" genes was validated by chromatin immunoprecipitation (ChIP)-RT-qPCR assays, using SD-grown, pTOC1::TOC1:YFP (TMG) (4) and pPIF3::YFP:PIF3 (YFP-PIF3) (5) seedlings, at post-dusk (ZT14) and dawn (ZT24), respectively. Each of these transgenes is driven by its own cognate native promoter and displays an expression pattern that recapitulates the corresponding endogenous pattern, as shown here for the diurnal pattern of TOC1 (SI Appendix, Fig. S2A,B), and as previously reported for PIF3 (5). The ZT14 and ZT24 time points are when each protein, respectively, is most abundant in the diurnal cycle (SI Appendix, Fig. S2A,B) (6). Compared to control samples, we observed robust enrichment of TOC1 and PIF3 in the promoter regions containing the binding sites previously identified by ChIP-seq (1, 2) (Fig. 1C).

To further explore the promoter binding dynamics in SD, we analyzed binding of both PIF3 and TOC1 to three of these dawn-phased PIF- and TOC1-bound genes (*PIL1*, *HFR1*, and *AT5G02580*), through the night (ZT8, ZT14, and ZT24) using the TMG and YFP-PIF3 lines. Maximum enrichment of TOC1 was detected at ZT14, and of PIF3 at ZT14 and ZT24 (Fig. 1D and SI Appendix, Fig. S2C), consistent with the abundance

patterns of the TOC1 (SI Appendix, Fig. S2B) and YFP-PIF3 (6) proteins under SD. Interestingly, the coincident binding of PIF3 and TOC1 to their co-bound promoters at ZT14 (Fig. 1D and SI Appendix, Fig. S2C), suggested to us that both proteins might be able to bind simultaneously to their co-targeted promoters post-dusk. To examine this possibility, we generated double transgenic TOC1ox/YFP-PIF3 plants over-expressing TOC1-MYC (2) in the YFP-PIF3 background (Note difference from TMG). These lines display a loss in TOC1 rhythmicity, maintaining constant amounts of TOC1 during the night in SD (2) (SI Appendix, Fig. S3A). In contrast to the TMG lines, the TOC1-ox protein showed a significant enrichment of promoter binding at ZT24, similar to the levels at ZT14 (Fig. 1E, and SI Appendix, Fig. S3B), consistent with previous results showing that TOC1 binding to its target promoters is dictated by its protein abundance (2). Overexpression of TOC1 did not significantly affect the abundance of YFP-PIF3 (SI Appendix, Fig. S3C), and promoter binding of PIF3 in the TOC1ox/YFP-PIF3 lines at ZT24 was comparable to that in the YFP-PIF3 line (Fig. 1F, and SI Appendix, Fig. S3D), further suggesting that binding of TOC1 and PIF3 to these promoters might take place simultaneously, rather than competitively.

CONTEXT: "The data show that the PIF and TOC1 binding sites lie within 120 bp for 74 % of the cobound genes and within 40 bp for 40% of these genes (Fig. 1G). These distances are consistent with concurrent, closely coincident DNA binding of the PIF and TOC1 proteins. A visual example of the high spatially coincident binding peaks for PIF3 and TOC1 is shown for *AT5G02580* in Fig. 1H. See *SI Appendix*, *SI Expanded Results* for the DNA motifs associated with PIF- and TOC1-bound genes." (Quoted from Main-text Results).

Candidate regulatory DNA motifs associated with PIF- and TOC1-bound genes

The groups of 49 "dawn-specific PIF-TOC1", 75 "No dawn-specific PIF-TOC1", 159 "TOC1-only", and 2,103 "PIF-only" gene subsets were analyzed for enrichment in DNA motifs using the SCOPE motif finder (http://genie.dartmouth.edu/scope/). Analysis was performed separately in sequences spanning 300 bp (+/- 150 bp) around the PIF- and the TOC1- associated peak maximum. The G-box and PBE/HUD binding elements were significantly present in all the gene sets bound by PIFs as expected (1, 7), with a

combined coverage of 100%, whereas in the "TOC1 only" the coverage was significantly reduced to 30.6%, and the PBE motif was not significantly present (Table S1). When interrogated for the presence of the previously described circadian motifs (ME, EE, PBX, EE-like, GATA, SBX, TBX) (8) we found that the ME and the PBX were specially enriched in the gene sets bound by PIFs compared to the "TOC1 only" genes, and that the % coverage was higher in the "dawn-specific PIF-TOC1" set compared to "No dawn-specific PIF-TOC1", specially for the PBX (Table S1). The putative TOC1 binding element T1ME (CACA) (9) was significantly present in all gene sets including the "PIF only", with a % coverage higher than 80% in all cases. Interestingly, a search for novel candidate regulatory motifs identified an "Extended G-box" (cacgtggg) and an "Extended PBE-box" (cacatggg) significantly and specifically enriched in the "dawn-specific PIF-TOC1" set around PIF binding sites (37.8% combined coverage) and TOC1 binding sites (26.5% combined coverage), compared to the "No dawn-specific PIF-TOC1" around PIF binding sites (13.9% combined coverage), "No dawn-specific PIF-TOC1" around TOC1 binding sites (10.1% combined coverage), "PIF only" (16.8% combined coverage), or "TOC1 only" (0% combined coverage) (Table S1). These data suggest that the extended G-box and PBE might confer specificity to drive dawn-specific expression under SD.

RESULTS SECTION: PIF3 and TOC1 interact and co-localize in the nucleus *in planta*.

CONTEXT: "Together, these results indicate that PIF3 and TOC1 can directly interact with each other in the nucleus under SD conditions. Binding-domain mapping shows that the C-terminal half of PIF3 is predominantly necessary for TOC1 binding (*SI Appendix, SI Expanded Results* and Fig. S4)." (Quoted from Main-text Results).

Binding-domain mapping of PIF3 interaction to TOC1

To map the domain(s) of PIF3 that binds to TOC1, we performed *in vitro* co-immunoprecipitation assays (10). By using a constant amount of full length GAD:PIF3 (FL) as bait, increased binding to TOC1 was observed with increasing amounts of TOC1 prey (Fig. 2C), indicative of direct PIF3-TOC1 binding. Using deletion variants of PIF3, we mapped the binding domain to the C-terminal half of the protein, with approximately

50% of the binding capacity residing in the bHLH domain (that mediates dimerization and binding to DNA), and 50% in the distal C-terminal end (Fig. 2C). By contrast, the N-terminal part of the protein containing the APA and APB motifs (that mediate PIF3 binding to phyA- and phyB-Pfr, respectively) appears to be dispensable (Fig. 2C). Previous domain interaction assays of TOC1 indicated that the N-terminal pseudoreceiver PR domain, shown to contain the transcriptional repression potential (9), is dispensable for binding to PIF3 (11), suggesting that TOC1 interaction with PIF3 is mediated through the intermediate (IR) region and/or the C-terminal CCT domain.

CONTEXT: "The data (Fig. 2C, and *SI Appendix*, Figs. S3 D and E) suggest that TOC1 likely binds DNA independently of PIF3, but the possibility that TOC1 binds through a different member of the PIF quartet cannot be discarded. Conversely, as described above for PIF3 promoter binding (Fig. 1F and *SI Appendix*, Fig. S3D), the data suggest that the interaction of TOC1 with PIF3 does not significantly affect PIF3 binding to DNA (See *SI Appendix*, *SI Expanded Results*)." (Quoted from Main-text Results).

PIF3 and TOC1 interaction does not significantly affect their binding to DNA

It has been reported that TOC1 can associate with DNA both directly through its CCT domain (9), and indirectly through interaction with DNA-binding factors (12). Because we have found that PIF3 and TOC1 interact and co-bind to the same regions of DNA, we addressed the possibility that PIF3 might be necessary to recruit TOC1 to the DNA. We generated TOC1-MYC overexpressing seedlings in a *pif3* background (TOC1ox/*pif3*) for comparison with TOC1ox/YFP-PIF3 seedlings (also in a *pif3* background). First, we found that PIF3 levels did not significantly affect TOC1 abundance (SI Appendix, Fig. S3D). Second, comparison of TOC1 binding to the promoters of *PIL1* and *HFR1* showed similar enrichment in SD-grown TOC1ox/YFP-PIF3 and *TOC1ox/pif3* seedlings (Fig. 2D). These results suggest that TOC1 likely binds DNA independently of PIF3. However, the possibility that TOC1 binds through a different PIF-quartet member cannot be discarded. Thus, our data are consistent with either possibility of direct or indirect binding of TOC1 to DNA. Conversely, as described above, we detected similar PIF3 enrichment levels in the promoters of *PIL1*, *HFR1* and *AT5G025780* both at ZT14 (when the levels of TOC1 are high) and ZT24 (when levels are low) (Fig. 1D, and SI Appendix,

Fig. S2C), and in WT and TOC1-OX backgrounds (Fig. 1F, and SI Appendix, Fig. S3D), suggesting, collectively, that the interaction of TOC1 with PIF3 does not significantly affect PIF3 binding to DNA. This finding is in contrast to other described PIF-interacting partners to date, like phyB, DELLAs, HFR1, and ELF3, which have been reported to inhibit binding of PIFs to DNA (13-17).

RESULTS SECTION: TOC1 represses PIF3 transcriptional activity in regulating pre-dawn-phased growth-related genes.

CONTEXT: "Previous evidence indicates that TOC1 can act as a transcriptional repressor (See *SI Appendix*, *SI Expanded Results*) (14, 16)." (Quoted from Main-text Results).

To begin to assess the possible repressor effect of TOC1 on PIF activity under SD, we examined whether TOC1 levels affect the diurnal pattern of dawn-phased, rising expression of their co-bound target genes in these conditions, by comparing expression of a selection of these genes in Col-0 and the TOC1-deficient mutant *toc1-101* (18). In all cases, we observed that the transcript levels in the *toc1* mutant were detected at ZT14-ZT16, several hours earlier than WT, where it occurred at ZT18-ZT20 (Fig. 3B and SI Appendix, Fig. S5). Expression in *toc1* continued to increase at this elevated level compared to WT throughout the rest of the night, peaking at dawn, and rapidly decreasing to almost undetectable levels after transition to light, similar to WT (Fig. 3B and SI Appendix, Fig. S5). This window of early expression in *toc1* (ZT14-ZT16) coincides with the time of highest TOC1 protein abundance in WT (Fig. 2B). This outcome cannot be attributed to *toc1* being a short-period mutant (19), because the early induction is not rescued under T21 conditions (SI Appendix, Fig. S6A), where a short day of 21 h (7 h day + 14 h night) matches the *toc1* internal short period. This is in contrast to the clock output gene, *CAB2,* that is early in *toc1* in a 24 h SD (T24 SD) but is rescued under a T21 SD (SI Appendix, Fig. S6A). Together, these data indicate that TOC1 prevents early expression of pre-dawn-phased genes that are directly induced by PIFs in SD. Because PIF3 transcript levels and PIF3 protein levels are not affected in *toc1* (SI Appendix, Fig. S7A-C), this result is consistent with TOC1 acting as a transcriptional repressor of PIF3, which itself acts intrinsically as a transcriptional

activator (20). Additionally, it suggests that, as PIF3 begins to progressively accumulate in the middle of the dark period in SD (ZT12-ZT16), its transcriptional regulatory activity is initially repressed by TOC1, thereby preventing early expression of PIF3 direct-target genes. Consistent with this suggestion, we found that the early (at ZT12-ZT16) *PIL1* expression observed in *toc1* compared to WT was suppressed in a *pif3toc1* mutant (Fig. 3B), providing strong evidence that the activity of endogenous PIF3 is repressed in the presence of TOC1 to limit early expression. We also observed that PIF4 and PIF5 removal in the *pif4pif5toc1* and *pif3pif4pif5toc1* mutants was able to partially suppress the expression of *PIL1* and *HFR1* (Fig. 3C). This result is consistent with TOC1 repression of the transcriptional activation activity of PIF4 and PIF5, as well as PIF3. However, because TOC1 directly represses the transcription of the *PIF4* and *PIF5* genes (SI Appendix, Fig. S9A and (2, 21)), this result might be at least partly attributed to higher PIF4 and PIF5 levels in the *toc1* mutant, in addition to, or instead of, reversal of TOC1 repression of the intrinsic transcriptional activation activity of the proteins. In addition, the effect of TOC1 removal on *PIL1* and *HFR1* was also observed at dawn under LD conditions (SI Appendix, Fig. S8A), where overall levels of expression are lower due to reduced accumulation of PIFs in the shorter dark period. This result suggests that the repressive action of TOC1 on PIF3 activity (and possibly other PIFs) takes place, not only under SD, but under other conditions where TOC1 and PIFs are both present.

Together, these data support the conclusion that TOC1 directly represses the intrinsic transcriptional activation activity of the PIF3 protein, and thus that PIF3 and TOC1 act antagonistically on the regulation of expression of their co-target genes under SD. We reasoned that it would then be expected that prolonged TOC1 activity during the night in TOC1ox seedlings should extend the repression of PIF3 activity beyond the ZT12-ZT16 time window. Strikingly consistent with this expectation, dark-induced expression of PIF3 target genes such as *HFR1* or *PIL1* is completely abolished in TOC1ox/YFP-PIF3, not only at ZT14 but also at ZT24 (Fig. 3D). Again, part of this effect might correspond to lower PIF4/5 abundance expected in TOC1ox lines compared to YFP-PIF3 (21). However, because we found that overexpression of TOC1 completely inhibits expression of the dawn-phased *PIL1* and *HFR1* genes without affecting the abundance or the DNA binding capacity of PIF3 (Fig. 1F, and SI Appendix, Fig. S7A-C), these results strongly

suggest that a major component of the effects of high TOC1 levels during the night in TOC1-over-expressing seedlings, is exerted by a sustained repressive action on the PIF3 protein (and possibly the other PIFs) during the dark period beyond ZT12-ZT16.

CONTEXT: "Consistent with a role of these ["predawn-specific PIF-TOC1"] genes in growth, gene ontology (GO) analysis shows enrichment for genes responsive to the growth-regulating hormones auxin, brassinosteroids, cytokinin, and gibberellin (*SI Appendix*, *SI Expanded Results* and Fig. S10)." (Quoted from Main-text Results).

Functional categorization of "pre-dawn-specific PIF-TOC1" genes

Consistent with a role of the "pre-dawn-specific PIF-TOC1" genes in growth, examination of these genes for gene ontology (GO) enrichment in biological processes revealed that in addition to categories related to responses to light (SI Appendix, Fig. S10), genes in the category of responses-to-endogenous-hormone stimuli were also highly enriched (SI Appendix, Fig. S10). These include hormone-associated genes involved in auxin (*HAT2*), brassinosteroid (*BRI1*), cytokinin (*CKX5*), and gibberellin (*GA2OX6*) pathways, suggesting that hormone gene expression might be antagonistically targeted by PIFs and TOC1 under SD photocycles. Interestingly, expression of the brassinosteroid receptor BRI1 has been previously proposed to reflect BRI1 activity, and more BRI1 expression correlated with increased hypocotyl growth (3). Diurnal rhythmic growth has also been described to involve regulation of auxin and gibberellin pathways (3, 22-25).

SI Discussion

Although the molecular data in the present work are mainly focused on PIF3, we suggest that our conclusions likely also apply to PIF1, PIF4 and PIF5, which promote growth during diurnal conditions together with PIF3, for the following reasons. First, PIF3, PIF4, and PIF5 deficiency collectively suppresses the elongated *toc1* phenotype under SD (Fig. 3C,F). Second, overexpression of TOC1 inhibits PIF-mediated gene expression to an extent that suggests repression not only of PIF3, but also of other PIFs (Fig. 3D). Third,

TOC1 can suppress skotomorphogenesis in the dark (Fig. 4A,B), which is mainly mediated by PIF1 (26). Finally, PIF1, PIF4, and PIF5 are also predicted to interact with TOC1 *in vivo* based on interaction assays in yeast (27). In the case of PIF4 and 5, the direct TOC1 transcriptional regulation of the *PIF4* and *PIF5* genes (2, 21, 28) prevents unequivocal interpretation of the genetic data presented here using *toc1* and *TOC1ox* seedlings. However, because comparison of PIF- and TOC1-bound genes shows overlap between TOC1 and all the PIF quartet members (Fig. 1A, Table S1), it is likely that both mechanisms (direct TOC1 repression of PIF4 and PIF5 protein activity, and regulation of *PIF4* and *PIF5* transcription) might occur concomitantly.

SI Material and Methods

Seedling growth and hypocotyl measurements. *Arabidopsis thaliana* seeds used in this manuscript include the previously described *pif3-3* (29), *pif4-2* (30), *pif5-3* (31), *pif4pif5* (32), *pif3pif4pif5* (26), *toc1-101* (18), pPIF3::YFP:PIF3 (YFP-PIF3) (5) and 35S::cMYC:TOC1 (TOC1ox) (2) in Col-0 ecotype, and *toc1-1* (19) and pTOC1::TOC1:YFP (TMG) (4) in C24 ecotype. The triple *pif4pif5toc1* and the quadruple *pif3pif4pif5toc1* mutants were generated by crossing *pif4pif5 and pif3pif4pif5* to *toc1-101* lines, respectively. The TOC1ox/YFP-PIF3 line was obtained by crossing 35S::cMYC:TOC1 and pPIF3::YFP:PIF3 lines.

Seed sterilization and stratification were done as previously described (6). Seedling growth was done in short days (8h light + 16h dark), long days (16h light + 8h dark) or continuous white light ($85\mu mol \cdot m^{-2} \cdot s^{-1}$) for the time indicated in each experiment. Saturating FR pulses were done as previously described (33). Hypocotyl measurements were done as in (29). For hypocotyl growth rate measurements, seedling growth and image acquisition were done as described (6).

Protein extraction and Immunoblots. Total protein extracts were obtained by resuspending grinded tissue samples in extraction buffer. Extraction buffer and protein quantification were done as described (30). Immunoblots to detect endogenous PIF3 and YFP-PIF3 proteins were done as in Soy et al. (2012) (6). Endogenous PIF3 was detected

using a PIF3 antibody (5). To detect TMG-YFP and MYC-TOC1 proteins, 80 µg of total protein were loaded to a 7.5% SDS-PAGE gel and immunodetection was performed using a rabbit polyclonal anti-GFP (Invitrogen) and a mouse monoclonal anti-cMYC (SIGMA), respectively. Peroxidase-linked anti-rabbit antibody (Amersham Biosciences) and anti-mouse antibody (Amersham Biosciences) were used as secondary antibodies to detect YFP and MYC, respectively. Detection was performed as described (6).

Chromatin Immunoprecipitation (ChIP) Assays. ChIP assays were performed as in Soy et al. (2012) (6). To analyze PIF3 binding in YFP-PIF3 and TOC1ox/YFP-PIF3 lines, immunoprecipitation was done overnight with GFP antibody-bound resin (GFP Agarose Beads, MBL). Mock ChIP reactions were performed with rProtein A-Sepharose (Bionova) without antibody to measure non-specific binding. To analyze TOC1 binding in lines TMG and TOC1ox/YFP-PIF3, samples were incubated overnight with rProtein A-Sepharose (Bionova) and anti-GFP polyclonal antibody (Invitrogen) or anti-cMYC antibody (Amersham Biosciences), respectively. Mock samples were processed without antibody. Purified DNA obtained at the end of the ChIP procedure was subjected to quantitative RT-PCR using promoter-specific primers for each gene (Table S2). Primer pairs were designed to span the region containing the G-box and/or the PBE predicted to be bound by the PIFs (1), and containing the predicted binding site for TOC1 (2). Both mock and antibody qRT-PCR results were first normalized to their common input and then fold enrichment was calculated for each antibody sample relative to the corresponding mock. *PP2A* (*AT1G13320*) enrichment was used for normalization. In ChIP experiments, seedlings at ZT8 were harvested and processed in the light, whereas seedlings and ZT14 and ZT24 were harvested and processed in the dark under green safelight.

Co-immunoprecipitation (CoIP) assay. *In planta* CoIP assays were performed as previously described (16) with some modifications. Briefly, 1 gr of fresh plant material was ground in 6 mL of CoIP extraction buffer [25mM Tris-HCl pH 8, 75mM NaCl, 0.5% of Nonidet P-40, 0.05 % Sodium Deoxycholate, 5mM β-mercaptoethanol, protease inhibitors (Roche complete tablets) and 50 µM MG132]. Homogenized was filtered with Miracloth filter and centrifuged at 13,000g for 15 min at 4°C. Supernatant was

transferred to a new tube, and 50 uL were saved as Input sample. The rest of the supernatant was incubated with 30 µL of anti-GFP magnetic beads (GFP-Trap, Chromotek) for 90 min at 4°C. Mock CoIP reactions were incubated with 30 µL of non-antibody magnetic beads (bmp-20, Chromotek). After incubation, beads were washed 3 times with CoIP extraction buffer and eluted by boiling the samples in 50 µL of Laemmli buffer for 15 min. Four CoIP eluates were mixed and loaded to a 7.5% SDS-PAGE gel as IP samples. Input samples were mixed with 15uL of Laemmli buffer and boiled for 15 min before loading. *In vitro* CoIP assays were performed as described (34) with the following modifications: paramagnetic beads (Dynal) were used for capture of the GAD tagged bait protein A, and washing was performed in the presence of 0.1% BSA. GAD:PIF3 and GAD:PIF3 deletions were as described (35). The coding region of *TOC1* was PCR-amplified from an Arabidopsis cDNA library with primers corresponding to the start and stop codons according to Makino et al. 2000 (36) and cloned into a 2xT7 driven phyA containing pBluescript vector (34) replacing the phyA open reading frame with TOC1.

Bimolecular Fluorescence Complementation assay. The coding regions of *PIF3* and *TOC1* were PCR-amplified and cloned into pGWnY and pGWcY vectors (37), respectively. The inner layers of spring onions were cut in 2 x 2 cm squares and used for particle bombardment. Each sample was transfected with 1 µg of each plasmid coupled to tungsten particles using a Biolistic Particle Delivery System PDS-1000 (Bio-Rad). After bombardment, onions were exposed to a saturating 15 min FR pulse and incubated overnight in dark conditions. The upper epidermal layer was removed, placed in a microscope slide and visualized using a confocal laser scanning microscope Olympus FV1000.

ChIP-Seq data analyses and visualization. To identify possible intervening genes, TOC1 peak-to-gene associations upstream of the 3'-end (2) were analyzed on data available at TAIR10 (ftp://ftp.arabidopsis.org/). All splicing variants for annotated genes were considered. The phases of expression were analyzed using the publicly available gene phase analysis tool PHASER (http://phaser.mocklerlab.org) (38) using a cutoff of 0.7. Transcript abundance of diurnal and circadian photocycles was analyzed using the

publicly available genome-wide expression data in DIURNAL (ftp://diurnal.mocklerlab.org) (38). Selected conditions were: SD (Col-0 SD), LD (longday), and Free Running (LL23_LDHH).

The Integrated Genome Browser (IGB) (39) was used to jointly visualize the ChIP-Seq data for TOC1 and PIFs alongside canonical gene models from TAIR10 (ftp://ftp.arabidopsis.org/).

PIF-TOC1 co-targets were functionally categorized to identify enriched Gene Ontology (GO) biological terms using the functional annotation classification system PANTHER through the Gene Ontology Consortium web page (http://geneontology.org/page/go-enrichment- analysis).

Distance between PIF and TOC1 peaks was calculated separately for all the different pair-wise combinations associated to the same peak. An average distance was then calculated for each peak and graphed in frequency intervals.

The SCOPE motif finder (http://genie.dartmouth.edu/scope/) was used to identify DNA motifs in sequences expanding 301 bp centered in the binding peak maximum determined for PIF and TOC1 for each AGI (1, 2). Sequences were searched to identify candidate regulatory DNA motifs, and also for the presence of previously defined PIF (7) and TOC1 (9) binding motifs, and diurnal and circadian modules (8).

SI Figure Legends

Fig. S1: Phase comparison of "PIF-TOC1", "PIF only", and "TOC1 only" gene sets under diurnal long-day conditions. Comparison of expression phases in long day of gene sets defined in Fig. 1A: 144 "PIF-TOC1" co-bound genes associated by both PIFs and TOC1 (green), 159 "TOC1 only" genes associated by TOC1 but not PIFs (blue), and 2,103 "PIF only" genes associated by PIFs but not by TOC1 (yellow). Phases as defined by PHASER (http://phaser.mocklerlab.org) are indicated on the circumference, and fold change phase enrichment of genes (count/expected) on the radius. The white and gray areas represent day and night, respectively.

Fig. S2: Time-course binding of TMG and PIF3 to *HFR1* and *AT5G02580* promoters under diurnal SD conditions. (A) Expression of TOC1-YFP under its endogenous promoter *(TMG)* analyzed by qRT-PCR in TMG seedling. *TMG* expression was normalized to *PP2A*. (B) Immunoblot analysis of TOC1-YFP protein in TMG seedlings. Protein extracts were probed with anti-GFP monoclonal antibody. Ponceau staining was used as a loading control. C24 ecotype is included as control. (C) ChIP analysis showing TOC1 and PIF3 binding to the *HFR1* and *AT5G02580* promoter in TMG (left) and YFP-PIF3 (right) seedlings, respectively. Samples were immunoprecipitated using anti-GFP antibody. Col-0 and C24 seedlings were used as WT control for YFP-PIF3 and TMG, respectively. Data are means from three technical replicates of one representative biological experiment. (A - C) Seedlings were grown under SD conditions for 2 days and samples were harvested during the third day of growth at the indicated time points.

Fig. S3: TOC1 and PIF3 levels and ChIP analysis of *HFR1* and *AT5G02580* promoters in the TOC1ox lines. (A) TOC1 protein levels in TOC1ox lines at ZT24 compared to ZT14. Immunoblot analysis of TOC1-MYC protein levels in TOC1-MYC/YFP-PIF3 lines (TOC1ox/YFP-PIF3). Protein extracts were probed with anti-MYC monoclonal antibody. Signal was quantified using the Multi Gauge V3.0 Image software in at least three independent biological replicates. Fold increase for each set was calculated considering one of the TOC1 values at ZT14 as 1. Error bars indicate SEM. Statistically significant differences between mean values were assayed by Student's *t* test. n.s.: not significant. (B) TOC1 overexpression extends to dawn the binding of TOC1 to the promoters of *HFR1* and *AT5G0258*. ChIP analysis shows TOC1 binding to the *HFR1* and *AT5G02580* promoter in the YFP-PIF3 and TOC1ox/YFP-PIF3 lines. Samples were immunoprecipitated using anti-MYC antibody. Data are means from three technical replicates of one representative biological experiment. (C) YFP-PIF3 protein levels are not affected by TOC1 overexpression. Immunoblot analysis of YFP-PIF3 protein in SD-grown YFP-PIF3 and TOC1ox/YFP-PIF3 seedlings. Protein extracts were probed with anti-PIF3 antibody to detect the YFP-PIF3 fusion. Ponceau staining was used as a loading control. A *pif3* mutant lacking PIF3 was used as a negative control. (D) TOC1 overexpression does not affect binding of PIF3 to *HFR1* and *AT5G02580*. ChIP analysis

shows PIF3 binding to the *HFR1* and *AT5G02580* promoter in SD-grown YFP-PIF3 and TOC1ox/YFP-PIF3. Samples were immunoprecipitated using anti-GFP antibody. Data are from two independent ChIP experiments, and error bars indicate SEM. (E) TOC1 protein levels in TOC1ox lines are not affected by PIF3 abundance. Samples were probed with anti-MYC monoclonal antibody to detect the TOC1-MYC fusion. Ponceau staining was used as a loading control. (A-E) Seedlings were grown under SD conditions for 2 days and samples were harvested during the third day of growth at the indicated time points.

Fig. S4. Mapping of the PIF3 binding domain responsible for interaction with TOC1. (Top) Schematic representation of the PIF3 domain structure showing the location of the binding sites for photoactivated phyB (APB) and phyA (APA), and the consensus bHLH domain. The deletion derivatives tested are indicated below. (Bottom left): Radiolabeled, in vitro-synthesized, full-length (FL) and C-terminal deletions of PIF3 (N402, N308, and N193) fused to GAD were used as bait to pull-down in vitro-synthesized TOC1. Autoradiograph showing binding of the various GAD:PIF3 derivatives to increasing amounts of TOC1. Approximately the same amount of bait was used for each construct in each tube. Expression level of all constructs was similar (data not shown). (Bottom right): Quantitative analysis of the data. The amount of each bait and prey used was calculated from a standard curve using a known amount of [35S] methionine. The femtomols of prey precipitated per femtomol of bait used are plotted against increasing amount of prey used.

Fig. S5. Expression analysis of "dawn-specific PIF-TOC1" genes under free-running conditions. Expression of *PIL1, HFR1, AT5G02580*, and *CAB2* was analyzed in Col-0 seedlings grown for 3 days in short day (SD) or for 2 days in SD followed by 1 day in continuous WL (SD+WL). Seedlings were harvested during the third day of growth. Expression was analyzed by qRT-PCR and values were normalized to *PP2A*. Data correspond to the average of three technical replicates of one representative biological experiment.

Fig. S6. TOC1 and PIF3 antagonistic regulation of dawn-phased growth-related genes in diurnal SD conditions. (A and B) Expression analysis of dawn-specific genes

by qRT-PCR in 3-day-old SD-grown Col-0 wild type, *toc1,* and *pif3pif4pif5* seedlings. Seedlings were grown for 2 days in SD conditions and samples were harvested at the indicated times during the third day of growth. Expression values were normalized to *PP2A*. (A) Expression of *HFR1*, *IAA19*, *AZF2*, *YUCCA8*, *IAA29*, *ATHB2*, *PAR1*, and *GA2OX6* was analyzed at ZT18 and ZT24. Data are the mean of 3 biological replicates. Different letters denote statistically significant differences among means by Tukey-b's test. (B) Expression of *AT5G02580*, *CKX5*, *FHL* and *HAT2* was analyzed through the third day of growth in SD.

Fig. S7. *toc1* phenotypes under a T21 photocycle. (A) Expression of *CAB2* and *PIL1* was analyzed in Col-0 and *toc1* seedlings grown for 3 days in 24 h short-day cycles (T24, 8h light and 16h dark) or in 21 h short-day cycles (T21, 7h light and 14h dark). Data are plotted as function of % of the diurnal cycle. Expression values were normalized to *PP2A*. When external period is matched to the internal short period of *toc1* (21 h), *CAB2* phenotype is rescued but *PIL1* is not. (B) Visual phenotype of Col-0 and *toc1* seedlings grown for 3 days in 21 h short-day cycles (T21). (C) Quantification of hypocotyl length of the seedlings shown in (B). Error bars indicate SEM of three independent studies with at least 25 seedlings each. The asterisk indicates statistically significant differences between mean values by Student's *t* test.

Fig. S8. Comparison of TOC1 and PIF regulation of *PIL1* and *HFR1* expression, and of seedling elongation, under SD and LD conditions. (A) Expression of *PIL1* (top) and *HFR1* (bottom) analyzed in 3 day-old long day (LD) and short day (SD) grown Col-0, *pif3*, *pif4*, *pif5*, *pif4pif5* (*pif45*), *pif3pif4pif5* (*pif345*), *toc1*, *pif3toc1*, *pif4pif5toc1* (*pif45toc1*), and *pif3pif4pif5toc1* (*pif345toc1*) seedlings at ZT23. Expression was analyzed by qRT-PCR and values were normalized to *PP2A*. (B and C) TOC1 and PIF3 antagonistically regulate growth in diurnal LD conditions. (B) Hypocotyl length of Col-0 wild-type, *toc1*, *pif345,* and *pif345toc1* seedlings grown for 3 days under continuous white light (WLc), LD, or SD conditions. (C) (Top) Visual phenotype of 3-day-old Col-0, *pif3*, *pif4*, *pif5*, *pif45*, *pif345*, *toc1*, *pif3toc1*, *pif45toc1*, and *pif345toc1* seedlings grown for 3 days in LD or SD conditions. (Bottom) Hypocotyl length of seedlings shown in top. Error bars indicate SEM of three independent studies with at least 25 seedlings each. (A-

C) Different letters denote statistically significant differences among means by Tukey-b's test. LD (upper case letters), SD (lower case letters), and WLc (lower case italics) data were processed independently.

Fig. S9. PIF levels in *toc1*. (A) *PIF4* and *PIF5* expression analysis in SD-grown Col-0 wild-type and *toc1* seedlings. (B) *PIF3* expression analysis in SD-grown Col-0 wild-type and *toc1* seedlings. (C) Immunoblots of protein extracts from 3-day-old Col-0 and *toc1* mutant seedlings. Seedlings were grown under SD conditions for 2 days and samples were harvested during the third day of growth at ZT18, ZT23 and ZT25. Extracts were probed using PIF3-specific polyclonal antibody. Ponceau staining was used as a loading control. (D) Quantification of PIF3 protein levels in SD-grown *toc1* mutant relative to Col-0. Seedlings were grown as in (C), and samples were harvested at ZT23. Data are the mean of 3 biological replicates. Error bars indicate SEM. Statistically significant differences between mean values were assayed by Student's *t* test. n.s.: not significant. In (A) and (B) seedlings were grown for 2 days in SD conditions and samples were harvested during the third day of growth at the indicated time points. Expression was analyzed by qRT-PCR and values were normalized to *PP2A*. (E) Hypocotyl elongation rate for Col-0 and *toc1* under SD conditions. Infrared imaging was used to monitor seedling growth from 2 day onwards every half an hour. Values are the mean of seven seedlings. Error bars indicate SEM. These data are shown in Fig. 2E as growth ratio difference between Col-0 and *toc1*.

Fig. S10. Functional categorization of the genes in the "dawn-specific PIF-TOC1" gene set. Functional classification of the 49 "dawn-specific PIF-TOC1" genes (defined in Fig. 1B and Supplementary Text) based on Biological Process was done using the gene ontology (GO) enrichment analysis tool (http://geneontology.org/page/go-enrichment-analysis). The figure shows the fold enrichment (count/expected) for the categories identified as significantly overrepresented (pvalue <0.5).

Fig. S11. Analysis of TOC1 gating of shade-stimulated PIF-mediated growth. (A) Diagram of the experimental design used for the gene expression experiment in Fig. 4D and 4E. Seedlings were grown for 2 days in SD conditions and were then released into continuous white light. A 15-min FR pulse (FRp) was given during the third day of

growth at the times indicated: CT8, CT14, CT18, and CT24. After the FRp, seedlings were kept in the dark for 15 min. Controls were harvested before the FRp. White, red, and black rectangles represent light, FRp, and darkness, respectively. (B) Immunoblot of endogenous PIF3 in Col-0 wild-type and *toc1* seedlings after the 15-min FRp given at CT8 and CT14 as described in (A). (C) Diagram of the experimental design used for the hypocotyl elongation experiment shown in Fig. 4F. Seedlings were grown for 2 days in SD conditions and were then released into continuous white light. A 15-min FRp was given during the third day of growth at the times indicated: CT8, CT14, CT18, and CT24. After the FRp, seedlings were kept in dark for 8 h. Controls were measured before the FRp. White, red, and black rectangles represent light, FRp, and darkness, respectively.

Fig. S12. Involvement of TOC1 in the regulation of hypocotyl elongation during seedling etiolation. Quantification of hypocotyl length in etiolated wild-type Col-0 and *toc1* seedlings. d: days in dark. Error bars indicate SEM.

Fig. S13. Phytochrome-photosensory and clock signaling pathways converge directly through shared binding to, and negative regulation of, PIF transcriptional activators. (Top) TOC1 and CCA1/LHY are part of the core clock oscillator in Arabidopsis and inhibit each other's transcription. TOC1 also connects directly to a set of output genes by repressing dark-induced, PIF-activated genes, during the early hours of diurnal darkness, through evening-phased accumulation of TOC1. (Bottom) Under short day conditions (SD), PIF-induced non-core-clock output genes of TOC1 sustain robust oscillations that peak at dawn. However, under free-running conditions of constant light (LL), where PIF levels are low due to phytochrome-mediated degradation, core-clock generated oscillations in TOC1 abundance lose the capacity to generate sustained entrained oscillations in LL (Fig. 3A and SI Appendix, Fig. S5), because PIF levels are too low to activate those genes.

SI References

1. Pfeiffer A, Shi H, Tepperman JM, Zhang Y, & Quail PH (2014) Combinatorial complexity in a transcriptionally centered signaling hub in Arabidopsis. *Molecular plant* 7(11):1598-1618.

2. Huang W*, et al.* (2012) Mapping the core of the Arabidopsis circadian clock defines the network structure of the oscillator. *Science* 336(6077):75-79.
3. Michael TP*, et al.* (2008) A morning-specific phytohormone gene expression program underlying rhythmic plant growth. *PLoS Biol* 6(9):e225.
4. Mas P, Alabadi D, Yanovsky MJ, Oyama T, & Kay SA (2003) Dual role of TOC1 in the control of circadian and photomorphogenic responses in Arabidopsis. *The Plant cell* 15(1):223-236.
5. Al-Sady B, Ni W, Kircher S, Schafer E, & Quail PH (2006) Photoactivated phytochrome induces rapid PIF3 phosphorylation prior to proteasome-mediated degradation. *Mol Cell* 23(3):439-446.
6. Soy J*, et al.* (2012) Phytochrome-imposed oscillations in PIF3 protein abundance regulate hypocotyl growth under diurnal light/dark conditions in Arabidopsis. *The Plant journal : for cell and molecular biology* 71(3):390-401.
7. Zhang Y*, et al.* (2013) A quartet of PIF bHLH factors provides a transcriptionally centered signaling hub that regulates seedling morphogenesis through differential expression-patterning of shared target genes in Arabidopsis. *PLoS Genet* 9(1):e1003244.
8. Michael TP*, et al.* (2008) Network discovery pipeline elucidates conserved time-of-day-specific cis-regulatory modules. *PLoS Genet* 4(2):e14.
9. Gendron JM*, et al.* (2012) Arabidopsis circadian clock protein, TOC1, is a DNA-binding transcription factor. *Proceedings of the National Academy of Sciences of the United States of America* 109(8):3167-3172.
10. Khanna R*, et al.* (2004) A novel molecular recognition motif necessary for targeting photoactivated phytochrome signaling to specific basic helix-loop-helix transcription factors. *The Plant cell* 16(11):3033-3044.
11. Makino S, Matsushika A, Kojima M, Yamashino T, & Mizuno T (2002) The APRR1/TOC1 quintet implicated in circadian rhythms of Arabidopsis thaliana: I. Characterization with APRR1-overexpressing plants. *Plant & cell physiology* 43(1):58-69.

12. Pruneda-Paz JL, Breton G, Para A, & Kay SA (2009) A functional genomics approach reveals CHE as a component of the Arabidopsis circadian clock. *Science* 323(5920):1481-1485.
13. de Lucas M*, et al.* (2008) A molecular framework for light and gibberellin control of cell elongation. *Nature* 451(7177):480-484.
14. Feng S*, et al.* (2008) Coordinated regulation of Arabidopsis thaliana development by light and gibberellins. *Nature* 451(7177):475-479.
15. Hornitschek P, Lorrain S, Zoete V, Michielin O, & Fankhauser C (2009) Inhibition of the shade avoidance response by formation of non-DNA binding bHLH heterodimers. *EMBO J* 28(24):3893-3902.
16. Nieto C, Lopez-Salmeron V, Daviere JM, & Prat S (2015) ELF3-PIF4 interaction regulates plant growth independently of the Evening Complex. *Current biology : CB* 25(2):187-193.
17. Park E*, et al.* (2012) Phytochrome B inhibits binding of phytochrome-interacting factors to their target promoters. *The Plant journal : for cell and molecular biology* 72(4):537-546.
18. Kikis EA, Khanna R, & Quail PH (2005) ELF4 is a phytochrome-regulated component of a negative-feedback loop involving the central oscillator components CCA1 and LHY. *The Plant journal : for cell and molecular biology* 44(2):300-313.
19. Somers DE, Webb AA, Pearson M, & Kay SA (1998) The short-period mutant, toc1-1, alters circadian clock regulation of multiple outputs throughout development in Arabidopsis thaliana. *Development* 125(3):485-494.
20. Al-Sady B, Kikis EA, Monte E, & Quail PH (2008) Mechanistic duality of transcription factor function in phytochrome signaling. *Proceedings of the National Academy of Sciences of the United States of America* 105(6):2232-2237.
21. Niwa Y, Yamashino T, & Mizuno T (2009) The circadian clock regulates the photoperiodic response of hypocotyl elongation through a coincidence mechanism in Arabidopsis thaliana. *Plant & cell physiology* 50(4):838-854.
22. Arana MV, Marin-de la Rosa N, Maloof JN, Blazquez MA, & Alabadi D (2011) Circadian oscillation of gibberellin signaling in Arabidopsis. *Proceedings of the*

National Academy of Sciences of the United States of America 108(22):9292-9297.

23. Kunihiro A*, et al.* (2011) Phytochrome-interacting factor 4 and 5 (PIF4 and PIF5) activate the homeobox ATHB2 and auxin-inducible IAA29 genes in the coincidence mechanism underlying photoperiodic control of plant growth of Arabidopsis thaliana. *Plant & cell physiology* 52(8):1315-1329.
24. Nomoto Y, Kubozono S, Yamashino T, Nakamichi N, & Mizuno T (2012) Circadian clock- and PIF4-controlled plant growth: a coincidence mechanism directly integrates a hormone signaling network into the photoperiodic control of plant architectures in Arabidopsis thaliana. *Plant & cell physiology* 53(11):1950-1964.
25. Nozue K, Harmer SL, & Maloof JN (2011) Genomic analysis of circadian clock-, light-, and growth-correlated genes reveals PHYTOCHROME-INTERACTING FACTOR5 as a modulator of auxin signaling in Arabidopsis. *Plant physiology* 156(1):357-372.
26. Leivar P*, et al.* (2008) Multiple phytochrome-interacting bHLH transcription factors repress premature seedling photomorphogenesis in darkness. *Current biology : CB* 18(23):1815-1823.
27. Yamashino T*, et al.* (2003) A Link between circadian-controlled bHLH factors and the APRR1/TOC1 quintet in Arabidopsis thaliana. *Plant & cell physiology* 44(6):619-629.
28. Nozue K*, et al.* (2007) Rhythmic growth explained by coincidence between internal and external cues. *Nature* 448(7151):358-361.
29. Monte E*, et al.* (2004) The phytochrome-interacting transcription factor, PIF3, acts early, selectively, and positively in light-induced chloroplast development. *Proceedings of the National Academy of Sciences of the United States of America* 101(46):16091-16098.
30. Leivar P*, et al.* (2008) The Arabidopsis phytochrome-interacting factor PIF7, together with PIF3 and PIF4, regulates responses to prolonged red light by modulating phyB levels. *The Plant cell* 20(2):337-352.

31. Khanna R*, et al.* (2007) The basic helix-loop-helix transcription factor PIF5 acts on ethylene biosynthesis and phytochrome signaling by distinct mechanisms. *The Plant cell* 19(12):3915-3929.
32. Leivar P*, et al.* (2012) Dynamic antagonism between phytochromes and PIF family basic helix-loop-helix factors induces selective reciprocal responses to light and shade in a rapidly responsive transcriptional network in Arabidopsis. *The Plant cell* 24(4):1398-1419.
33. Soy J, Leivar P, & Monte E (2014) PIF1 promotes phytochrome-regulated growth under photoperiodic conditions in Arabidopsis together with PIF3, PIF4, and PIF5. *Journal of experimental botany* 65(11):2925-2936.
34. Zhu Y, Tepperman JM, Fairchild CD, & Quail PH (2000) Phytochrome B binds with greater apparent affinity than phytochrome A to the basic helix-loop-helix factor PIF3 in a reaction requiring the PAS domain of PIF3. *Proceedings of the National Academy of Sciences of the United States of America* 97(24):13419-13424.
35. Ni M, Tepperman JM, & Quail PH (1998) PIF3, a phytochrome-interacting factor necessary for normal photoinduced signal transduction, is a novel basic helix-loop-helix protein. *Cell* 95(5):657-667.
36. Makino S*, et al.* (2000) Genes encoding pseudo-response regulators: insight into His-to-Asp phosphorelay and circadian rhythm in Arabidopsis thaliana. *Plant & cell physiology* 41(6):791-803.
37. Tanaka Y*, et al.* (2012) *Gateway Vectors for Plant Genetic Engineering: Overview of Plant Vectors, Application for Bimolecular Fluorescence Complementation (BiFC) and Multigene Construction* (InTech, ISBN: 978-953-307-790-1).
38. Mockler TC*, et al.* (2007) The DIURNAL project: DIURNAL and circadian expression profiling, model-based pattern matching, and promoter analysis. *Cold Spring Harbor symposia on quantitative biology* 72:353-363.
39. Nicol JW, Helt GA, Blanchard SG, Jr., Raja A, & Loraine AE (2009) The Integrated Genome Browser: free software for distribution and exploration of genome-scale datasets. *Bioinformatics* 25(20):2730-2731.

Table S1. Motifs associated with PIF and TOC1 ChIP-Seq target genes

Presence of previously described diurnal and circadian DNA motifs (8) for association with PIF and TOC1 binding sites (+/- 150 bp) in the "dawn-specific PIF-TOC1" and "No dawn-specific PIF-TOC1" (as defined in Results and Dataset 1) for both PIF and TOC1 associated peaks analyzed separately, and in the "PIF only" and "TOC1 only" gene sets, as defined in Figure 1. Analyses were performed using the SCOPE motif finder (http://genie.dartmouth.edu/scope/). Base pair "r" refers to either "g" or "a". Highlighted in green are the top-scoring significant motifs (Significance >0) with percentage coverage greater than 20%. The "Extended G-box" (cacgtggg) and "Extended PBE" (cacatggg) correspond to *de novo* defined motifs.

"Dawn-specific PIF-TOC1" genes. PIF-associated peaks.

	MOTIF	SIGNIFICANCE	% COVERAGE
G-box	cacgtg	386	69.3%
PBE/HUD	cacatg	89.7	52%
G-box+PBE	cacrtg	426.7	100%
T1ME	caca	26.9	94.5%
ME	ccacac	20.3	22.8%
PBX	atgggcc	44.5	30.7%
EE	aaaatatct	-15	3.9%
EE-like	aatatct	-12	11.8%
GATA	ggata	-3.8	40.2%
SBX	aagccc	-9.4	14.2%
TBX	aaaccct	-12.1	0%
Extended G-box	cacgtggg	157	25%
Extended PBE	cacatggg	39.8	12.6%
Extended G-box+PBE	cacrtggg	202.9	37.8%

“No dawn-specific PIF-TOC1” genes. PIF-associated peaks.

	MOTIF	SIGNIFICANCE	% COVERAGE
G-box	cacgtg	600	83%
PBE/HUD	cacatg	33	34%
G-box+PBE	cacrtg	499	100%
T1ME	caca	16	83%
ME	ccacac	18.6	20%
PBX	atgggcc	0.4	13.3%
EE	aaaatatct	-10.9	6.1%
EE-like	aatatct	3.3	20%
GATA	ggata	6.3	46.7%
SBX	aagccc	0.5	20.6%
TBX	aaaccct	-13.0	6.1%
Extended G-box	cacgtggg	55	12.7%
Extended PBE	cacatggg	-12.6	1.2%
Extended G-box+PBE	cacrtggg	44	13.9%

“PIF only” genes

	MOTIF	SIGNIFICANCE	% COVERAGE
G-box	cacgtg	1063	64.2%
PBE/HUD	cacatg	1063	53.8%
G-box+PBE	cacrtg	1062.4	99.6%
T1ME	caca	756.6	94.2%
ME	ccacac	188	16.8%
PBX	atgggcc	11.5	9.0%
EE	aaaatatct	-16.4	2.3%
EE-like	aatatct	-12.8	10.4%
GATA	ggata	13.3	36.4%
SBX	aagccc	-11	9.8%
TBX	aaaccct	-13	5.5%
Extended G-box	cacgtggg	791.4	10.7%
Extended PBE	cacatggg	367.4	6.5%
Extended G-box+PBE	cacrtggg	1058.4	16.8%

“dawn-specific PIF-TOC1” genes. TOC1-associated peaks.

	MOTIF	SIGNIFICANCE	% COVERAGE
G-box	cacgtg	124.9	71.4%
PBE/HUD	cacatg	14.8	44.9%
G-box+PBE	cacrtg	123.4	91.8%
T1ME	caca	3	95.9%
ME	ccacac	-2.9	16.3%
PBX	atgggcc	0	22.4%
EE	aaaatatct	-16.5	2%
EE-like	aatatct	-12.8	8.2%
GATA	ggata	-6.8	36.7%
SBX	aagccc	-10.9	6.1%
TBX	aaaccct	-12.9	0%
Extended G-box	cacgtggg	27.1	16.3%
Extended PBE	cacatggg	2.5	10.2%
Extended G-box+PBE	cacrtggg	40.8	26.5%

“No dawn-specific PIF-TOC1” genes. TOC1-associated peaks.

	MOTIF	SIGNIFICANCE	% COVERAGE
G-box	cacgtg	211.5	72.2%
PBE/HUD	cacatg	-4.1	22.8%
G-box+PBE	cacrtg	147.5	79.7%
T1ME	caca	10.4	88.6%
ME	ccacac	-1.5	16.5%
PBX	atgggcc	1.5	19.0%
EE	aaaatatct	-16.3	2.5%
EE-like	aatatct	-11.0	13.9%
GATA	ggata	-2.1	43.0%
SBX	aagccc	-7.8	16.5%
TBX	aaaccct	-12.5	1.3%
Extended G-box	cacgtggg	7.2	8.9%
Extended PBE	cacatggg	-13.3	1.3%
Extended G-box+PBE	cacrtggg	3.7	10.1%

“TOC1 only” genes

	MOTIF	SIGNIFICANCE	% COVERAGE
G-box	cacgtg	31.3	24.8%
PBE/HUD	cacatg	-10.5	8.3%
G-box+PBE	cacrtg	4.6	30.6%
T1ME	caca	24.7	91.7%
ME	ccacac	11.3	19.7%
PBX	atgggcc	-2.0	13.4%
EE	aaaatatct	-16.2	2.5%
EE-like	aatatct	-8.6	14.0%
GATA	ggata	-7.2	35.7%
SBX	aagccc	-6.1	15.9%
TBX	aaaccct	-13	6.4%
Extended G-box	cacgtggg	-15	0%
Extended PBE	cacatggg	-15	0%
Extended G-box+PBE	cacrtggg	-15.6	0%

Table S2. List of Oligonucleotides

Name	AGI number	Gene Region	Primers	
			Name	Sequence (from 5' to 3')
PIL1	*AT2G46970*	Promoter	EMP407 (PIF3)	ACAAGAAAGAAGGGAGGGAGACA
			EMP408 (PIF3)	TTCTCTTTAAATGGGACCCACAAT
			EMP550 (TOC1)	GGACGCTTTGTCATTGCATAG
			EMP551 (TOC1)	GATGCTCCAACAATAATGCAAC
		Coding region	EMP372	TGCCTTCGTGTGTTTCTCAG
			EMP373	AACTAAAACCGTTGCTTCCTC
HFR1	*AT1G02340*	Promoter	EMP444 (PIF3)	ACGTGATGCCCTCGTGATGGAC
			EMP445 (PIF3)	GTCGCTCGCTAAGACACCAAC
			EMP626 (TOC1)	TGAACAGTGGGAAGTTGTAGATTG
			EMP444 (TOC1)	ACGTGATGCCCTCGTGATGGAC
		Coding region	EMP448	GATGCGTAAGCTACAGCAACTCGT
			EMP449	AGAACCGAAACCTTGTCCGTCTTG
AT5G02580	*AT5G02580*	Promoter	EMP618	ACAGATTTTAACTACGTAGTGTGGG
			EMP619	TGCTACTGCTAGTATCAGTTGCTG
		Coding region	EMP582	CAAAGAGTTCTTCGAGGCATACG
			EMP583	TAGTTCGTGAAAGCAAATCACGG
FHL	*AT5G02200*	Promoter	EMP620	GTCAGGGCCCACAATAGTCTCAC
			EMP810	CAAATCCGCGTTCTCAACC
		Coding region	EMP584	TGGAGAACACAAAAACCAGCGATGA
			EMP585	TCAATGGTTGGTTTCGTGGTAGCTT
HAT2	*AT5G47370*	Promoter	EMP905	AAGTAGGCAGCAGTTAAAGGAATC
			EMP906	TGAGCAATATTGGTCAAGTGTGTG
		Coding region	EMP592	GACTCCCATGGAACCAAACATTCG
			EMP593	CTCTTCCCGCTAATGGTGCTTGA

CKX5	*AT1G75450*	Promoter	EMP901	GAGTTTGTGTTATTACCGTGCAAG
			EMP902	GATAAATAGAGTCATGGGGAGAGG
		Coding region	EMP586	ACTCGAGCACGAATCTCTCTCGAAC
			EMP587	CGAGTCCTTCGTCCACAATCACAA
GA2OX6	*AT1G02400*	Promoter	EMP907	AAGTGGGTAGGTACTAGGTATTGG
			EMP908	GAAAAGAGTCACAAGGAAGTGGG
		Coding region	EMP783	GGTTGAATCACTATCCACCAGC
			EMP784	TAACGGTGGAGCTGCAAAGTAC
PAR1	*AT2G42870*	Promoter	EMP801	AAGGACAGATTTAGGAGGTCACTG
			EMP802	GTGAACTTGTTCGTACAATTGAGG
		Coding region	EMP715	CACCGTCATGCTCAGCCA
			EMP716	TCGGTCTTCACGTACGCTTG
IAA19	*AT3G15540*	Coding region	EMP689	AGATGAATATGACGTCGTCGG
			EMP690	CTCAACCTCTTGCATGACTCTAG
AZF2	*AT3G26810*	Coding region	EMP701	CAAGTATGAAACAATGCGATCCCTTTG
			EMP702	TTCTTCCATCCGGTTATTATCATTCTCG
YUCCA8	*AT4G28720*	Coding region	EMP709	ATCAACCCTAAGTTCAACGAGTG
			EMP710	CTCCCGTAGCCACCACAAG
IAA29	*AT4G32280*	Coding region	EMP711	ATCACCATCATTGCCCGTAT
			EMP712	ATTGCCACACCATCCATCTT
ATHB2	*AT4G16780*	Coding region	EMP713	GAGGTAGACTGCGAGTTCTTACG
			EMP714	GCATGTAGAACTGAGGAGAGAGC
TOC1	*AT5G61380*	Coding region	EMP415	TCTTCGCAGAATCCCTGTGAT
			EMP416	GCTGCACCTAGCTTCAAGCA
PIF3	*AT1G09530*	Coding region	EMP417	GGTATGGGAATGCCTTATGCA
			EMP418	TGGAACTGTGGTCCGTGGTTA
PIF4	*AT2G43010*	Coding region	EMP419	GCGGCTTCGGCTCCGATGAT
			EMP420	AGTCGCGGCCTGCATGTGTG

PIF1	*AT2G20180*	Coding region	EMP540	ATCCAACCTCGGGCCAGCCT
			EMP541	TTGGGTCGGGTGGAGACCGC
CAB2	*AT1G29920*	Coding region	EMP474	CTATTTCTACAATCGAGCAACGTGA
			EMP475	TGTACCCATTGCCTTAATATGTTCAA
PP2A	*AT1G13320*	Coding region	EMP338	TATCGGATGACGATTCTTCGTGCAG
			EMP339	GCTTGGTCGACTATCGGAATGAGAG

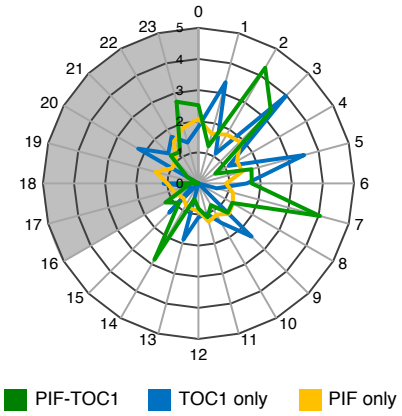

Fig. S1: Phase comparison of "PIF-TOC1", "PIF only", and "TOC1 only" gene sets under diurnal long-day conditions. Comparison of expression phases in long day of gene sets defined in Fig. 1A: 144 "PIF-TOC1" co-bound genes associated by both PIFs and TOC1 (green), 159 "TOC1 only" genes associated by TOC1 but not PIFs (blue), and 2103 "PIF only" genes associated by PIFs but not by TOC1 (yellow). Phases as defined by PHASER (http://phaser.mocklerlab.org) are indicated on the circumference, and fold change phase enrichment of genes (count/expected) on the radius. The white and gray areas represent day and night, respectively.

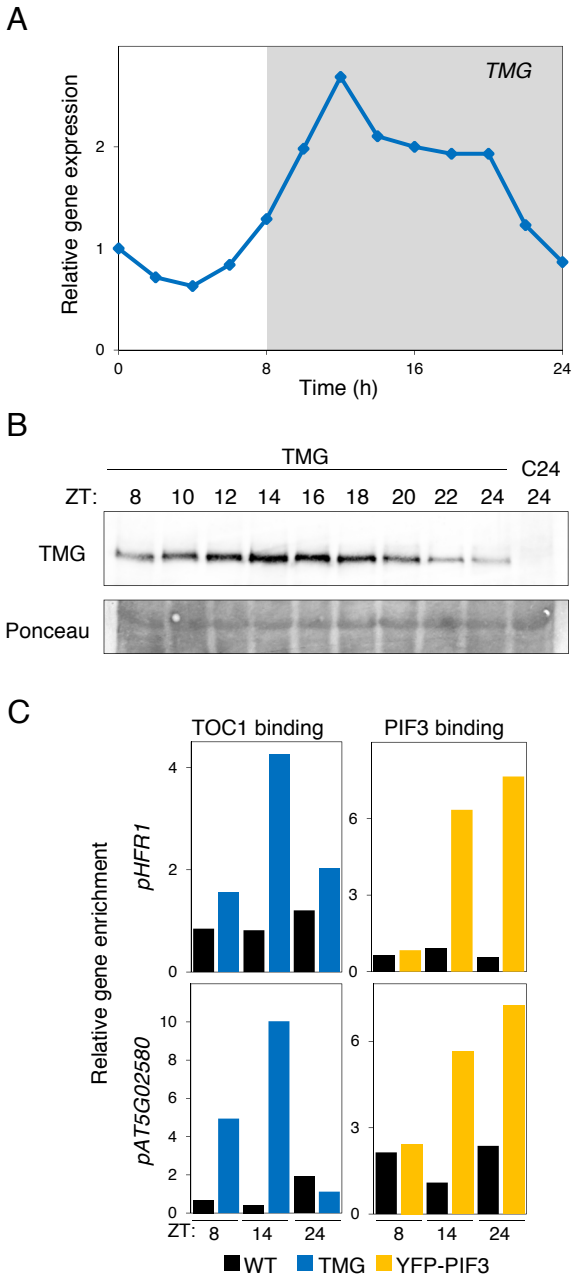

Fig. S2: Time-course binding of TMG and PIF3 to *HFR1* and *AT5G02580* promoters under diurnal SD conditions. (A) Expression of TOC1-YFP under its endogenous promoter *(TMG)* analyzed by qRT-PCR in TMG seedling. *TMG* expression was normalized to *PP2A*. (B) Immunoblot analysis of TOC1-YFP protein in TMG seedlings. Protein extracts were probed with anti-GFP monoclonal antibody. Ponceau staining was used as a loading control. C24 ecotype is included as control. (C) ChIP analysis showing TOC1 and PIF3 binding to the *HFR1* and *AT5G02580* promoter in TMG (left) and YFP-PIF3 (right) seedlings, respectively. Samples were immunoprecipitated using anti-GFP antibody. Col-0 and C24 seedlings were used as WT control for YFP-PIF3 and TMG, respectively. Data are means from three technical replicates of one representative biological experiment. (A - C) Seedlings were grown under SD conditions for 2 days and samples were harvested during the third day of growth at the indicated time points.

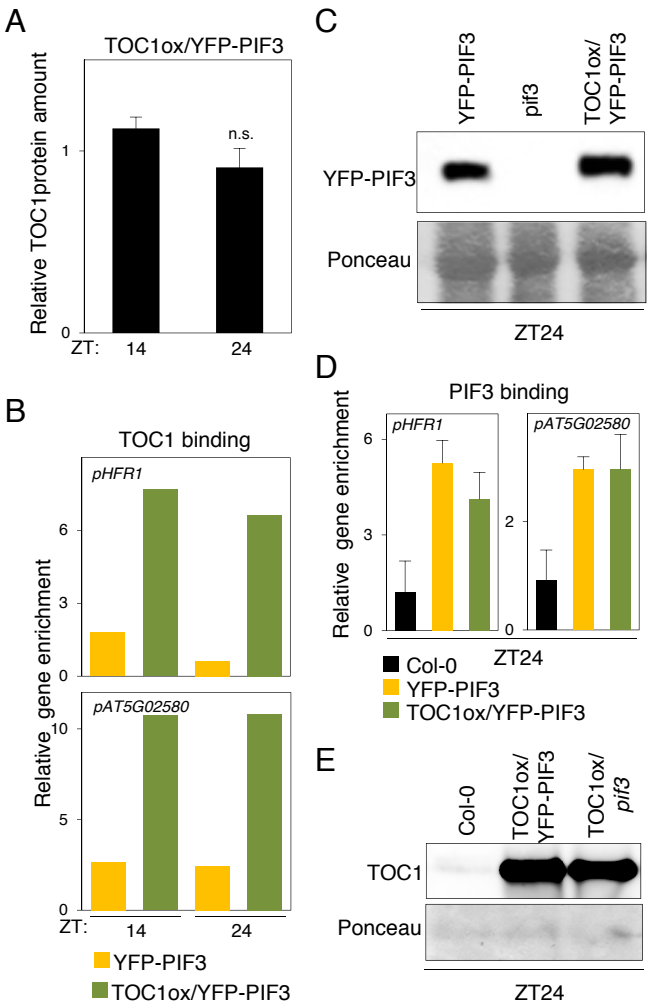

Fig. S3: TOC1 and PIF3 levels and ChIP analysis of *HFR1* and *AT5G02580* promoters in the TOC1ox lines. (A) TOC1 protein levels in TOC1ox lines at ZT24 compared to ZT14. Immunoblot analysis of TOC1-MYC protein levels in TOC1-MYC/YFP-PIF3 lines (TOC1ox/YFP-PIF3). Protein extracts were probed with anti-MYC monoclonal antibody. Signal was quantified using the Multi Gauge V3.0 Image software in at least three independent biological replicates. Fold increase for each set was calculated considering one of the TOC1 values at ZT14 as 1. Error bars indicate SEM. Statistically significant differences between mean values were assayed by Student's *t* test. n.s.: not significant. (B) TOC1 overexpression extends to dawn the binding of TOC1 to the promoters of *HFR1* and *AT5G0258*. ChIP analysis shows TOC1 binding to the *HFR1* and *AT5G02580* promoter in the YFP-PIF3 and TOC1ox/YFP-PIF3 lines. Samples were immunoprecipitated using anti-MYC antibody. Data are means from three technical replicates of one representative biological experiment. (C) YFP-PIF3 protein levels are not affected by TOC1 overexpression. Immunoblot analysis of YFP-PIF3 protein in SD-grown YFP-PIF3 and TOC1ox/YFP-PIF3 seedlings. Protein extracts were probed with anti-PIF3 antibody to detect the YFP-PIF3 fusion. Ponceau staining was used as a loading control. A *pif3* mutant lacking PIF3 was used as a negative control. (D) TOC1 overexpression does not affect binding of PIF3 to *HFR1* and *AT5G02580*. ChIP analysis shows PIF3 binding to the *HFR1* and *AT5G02580* promoter in SD-grown YFP-PIF3 and TOC1ox/YFP-PIF3. Samples were

immunoprecipitated using anti-GFP antibody. Data are from two independent ChIP experiments, and error bars indicate SEM. (E) TOC1 protein levels in TOC1ox lines are not affected by PIF3 abundance. Samples were probed with anti-MYC monoclonal antibody to detect the TOC1-MYC fusion. Ponceau staining was used as a loading control. (A-E) Seedlings were grown under SD conditions for 2 days and samples were harvested during the third day of growth at the indicated time points.

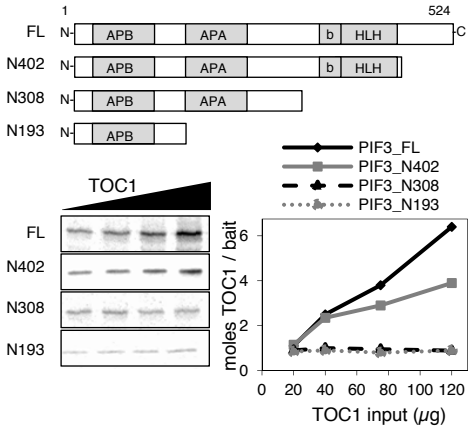

Fig. S4. Mapping of the PIF3 binding domain responsible for interaction with TOC1. (Top) Schematic representation of the PIF3 domain structure showing the location of the binding sites for photoactivated phyB (APB) and phyA (APA), and the consensus bHLH domain. The deletion derivatives tested are indicated below. (Bottom left): Radiolabeled, in vitro-synthesized, full-length (FL) and C-terminal deletions of PIF3 (N402, N308, and N193) fused to GAD were used as bait to pull-down in vitro-synthesized TOC1. Autoradiograph showing binding of the various GAD:PIF3 derivatives to increasing amounts of TOC1. Approximately the same amount of bait was used for each construct in each tube. Expression level of all constructs was similar (data not shown). (Bottom right): Quantitative analysis of the data. The amount of each bait and prey used was calculated from a standard curve using a known amount of [35S] methionine. The femtomols of prey precipitated per femtomol of bait used are plotted against increasing amount of prey used.

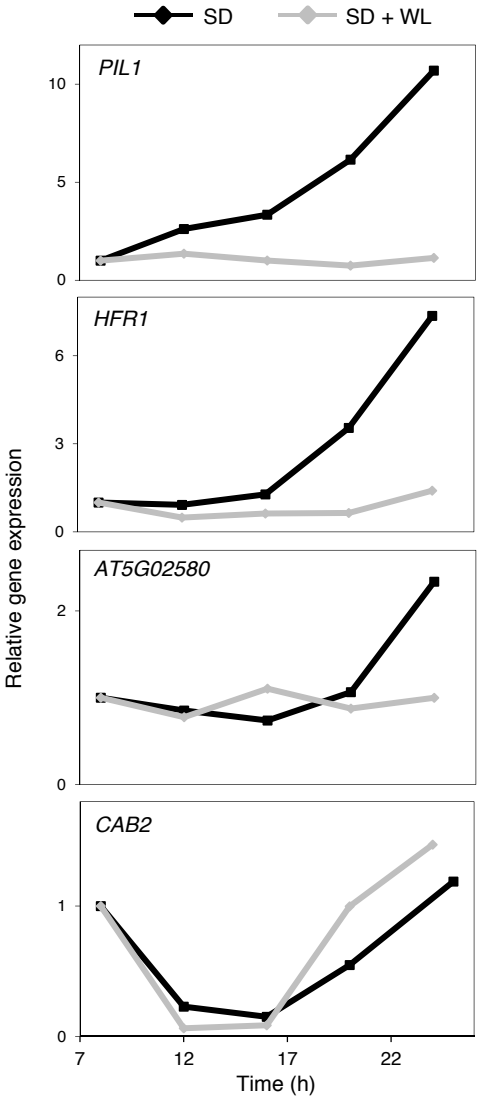

Fig. S5. Expression analysis of "dawn-specific PIF-TOC1" genes under free-running conditions. Expression of *PIL1*, *HFR1*, *AT5G02580*, and *CAB2* was analyzed in Col-0 seedlings grown for 3 days in short day (SD) or for 2 days in SD followed by 1 day in continuous WL (SD+WL). Seedlings were harvested during the third day of growth. Expression was analyzed by qRT-PCR and values were normalized to *PP2A*. Data correspond to the average of three technical replicates of one representative biological experiment.

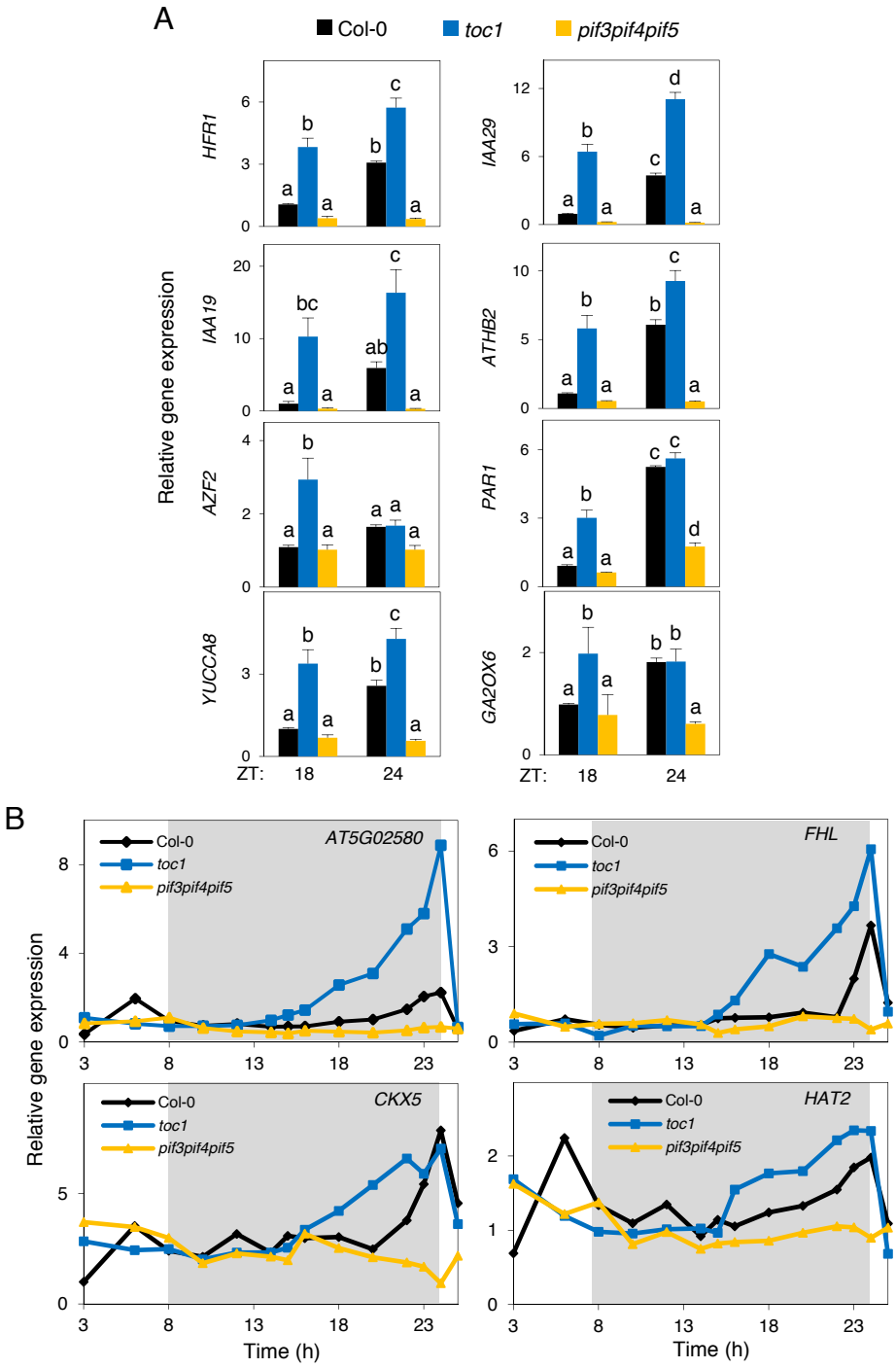

Fig. S6. TOC1 and PIF3 antagonistic regulation of dawn-phased growth-related genes in diurnal SD conditions. (A and B) Expression analysis of dawn-specific genes by qRT-PCR in 3-day-old SD-grown Col-0 wild type, *toc1*, and *pif3pif4pif5* seedlings. Seedlings were grown for 2 days in SD conditions and samples were harvested at the indicated times during the third day of growth. Expression values were normalized to *PP2A*. (A) Expression of *HFR1*, *IAA19*, *AZF2*, *YUCCA8*, *IAA29*, *ATHB2*, *PAR1*, and *GA2OX6* was analyzed at ZT18 and ZT24. Data are the mean of 3 biological replicates. Different letters denote statistically significant differences among means by Tukey-b's test. (B) Expression of *AT5G02580*, *CKX5*, *FHL* and *HAT2* was analyzed through the third day of growth in SD.

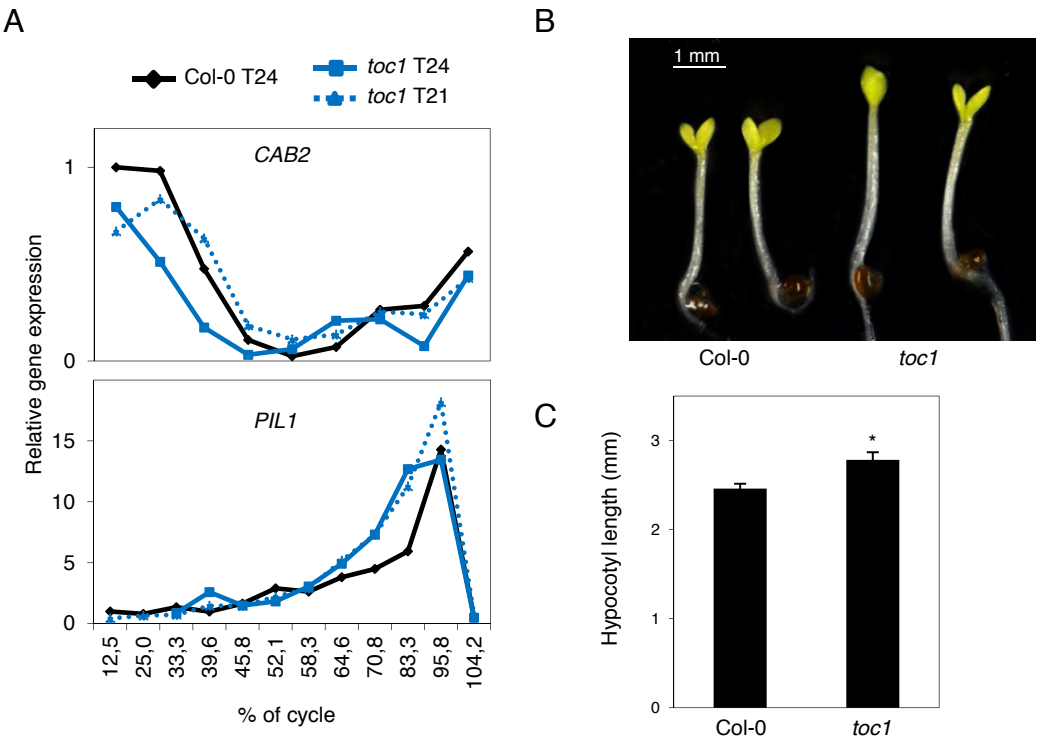

Fig. S7. *toc1* phenotypes under a T21 photocycle. (A) Expression of *CAB2* and *PIL1* was analyzed in Col-0 and *toc1* seedlings grown for 3 days in 24 h short-day cycles (T24, 8h light and 16h dark) or in 21 h short-day cycles (T21, 7h light and 14h dark). Data are plotted as function of % of the diurnal cycle. Expression values were normalized to *PP2A*. When external period is matched to the internal short period of *toc1* (21 h), *CAB2* phenotype is rescued but *PIL1* is not. (B) Visual phenotype of Col-0 and *toc1* seedlings grown for 3 days in 21 h short-day cycles (T21). (C) Quantification of hypocotyl length of the seedlings shown in (B). Error bars indicate SEM of three independent studies with at least 25 seedlings each. The asterisk indicates statistically significant differences between mean values by Student's *t* test.

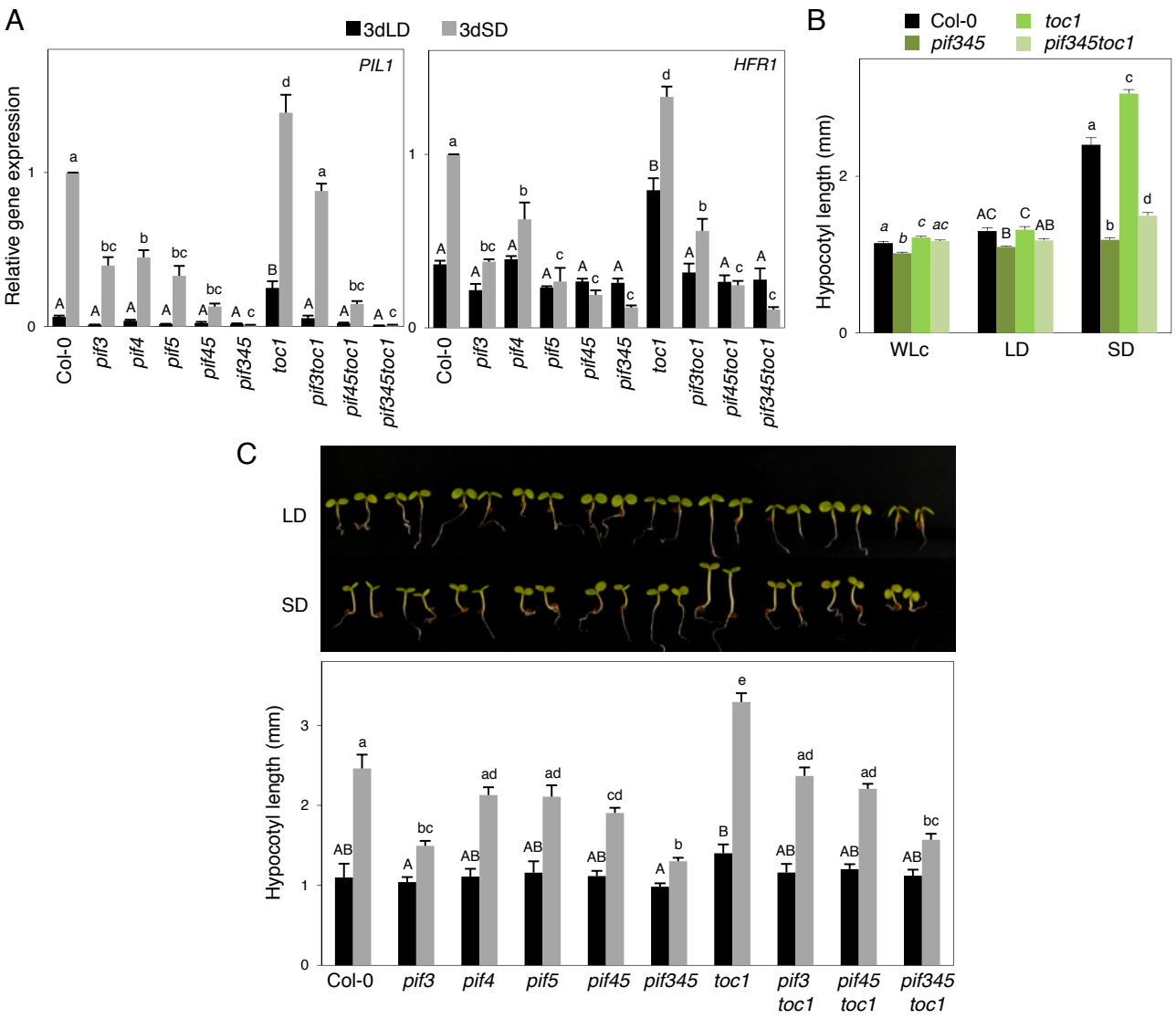

Fig. S8. Comparison of TOC1 and PIF regulation of PIL1 and HFR1 expression, and of seedling elongation, under SD and LD conditions. (A) Expression of PIL1 (top) and HFR1 (bottom) analyzed in 3 day-old long day (LD) and short day (SD) grown Col-0, *pif3*, *pif4*, *pif5*, *pif4pif5* (*pif45*), *pif3pif4pif5* (*pif345*), *toc1*, *pif3toc1*, *pif4pif5toc1* (*pif45toc1*), and *pif3pif4pif5toc1* (*pif345toc1*) seedlings at ZT23. Expression was analyzed by qRT-PCR and values were normalized to PP2A. (B and C) TOC1 and PIF3 antagonistically regulate growth in diurnal LD conditions. (B) Hypocotyl length of Col-0 wild-type, *toc1*, *pif345*, and *pif345toc1* seedlings grown for 3 days under continuous white light (WLc), LD, or SD conditions. (C) (Top) Visual phenotype of 3-day-old Col-0, *pif3*, *pif4*, *pif5*, *pif45*, *pif345*, *toc1*, *pif3toc1*, *pif45toc1*, and *pif345toc1* seedlings grown for 3 days in LD or SD conditions. (Bottom) Hypocotyl length of seedlings shown in top. Error bars indicate SEM of three independent studies with at least 25 seedlings each. (A-C) Different letters denote statistically significant differences among means by Tukey-b's test. LD (upper case letters), SD (lower case letters), and WLc (lower case italics) data were processed independently.

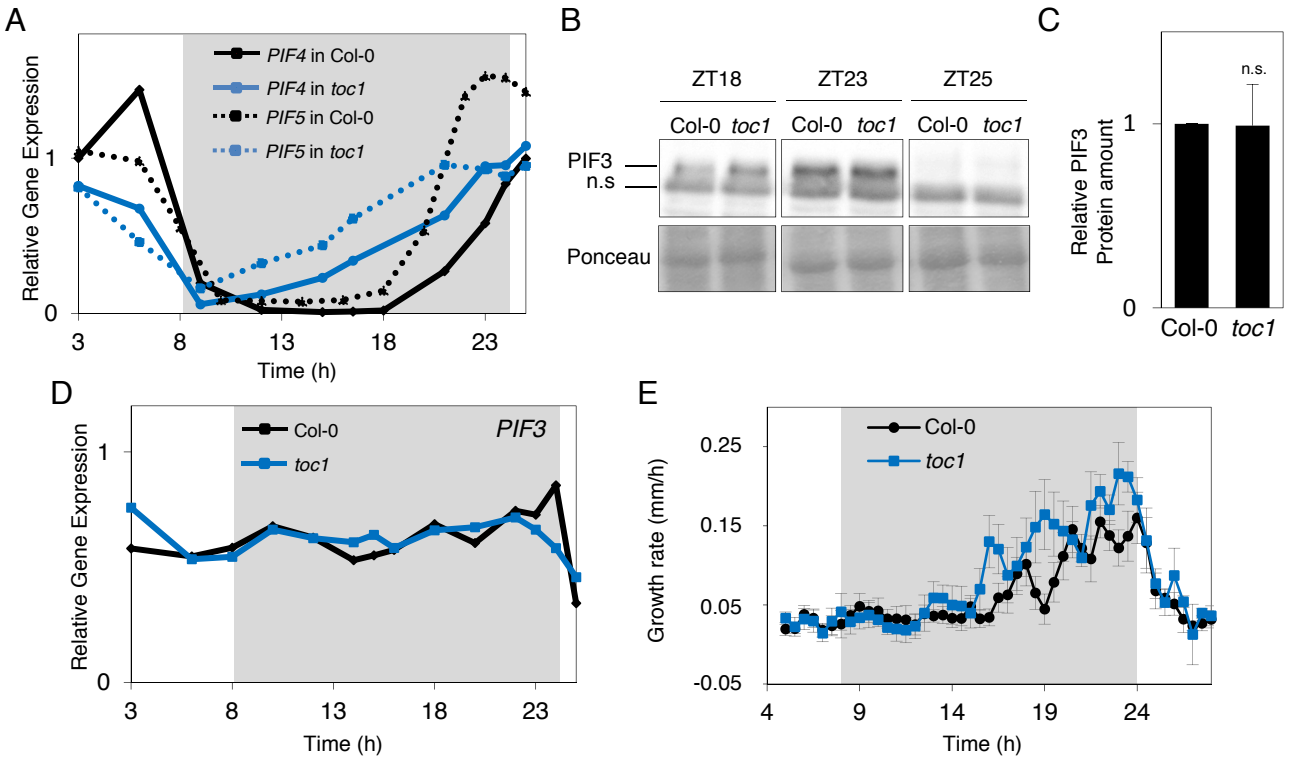

Fig. S9. PIF levels in *toc1*. (A) *PIF4* and *PIF5* expression analysis in SD-grown Col-0 wild-type and *toc1* seedlings. (B) *PIF3* expression analysis in SD-grown Col-0 wild-type and *toc1* seedlings. (C) Immunoblots of protein extracts from 3-day-old Col-0 and *toc1* mutant seedlings. Seedlings were grown under SD conditions for 2 days and samples were harvested during the third day of growth at ZT18, ZT23 and ZT25. Extracts were probed using PIF3-specific polyclonal antibody. Ponceau staining was used as a loading control. (D) Quantification of PIF3 protein levels in SD-grown *toc1* mutant relative to Col-0. Seedlings were grown as in (C), and samples were harvested at ZT23. Data are the mean of 3 biological replicates. Error bars indicate SEM. Statistically significant differences between mean values were assayed by Student's *t* test. n.s.: not significant. In (A) and (B) seedlings were grown for 2 days in SD conditions and samples were harvested during the third day of growth at the indicated time points. Expression was analyzed by qRT-PCR and values were normalized to *PP2A*. (E) Hypocotyl elongation rate for Col-0 and *toc1* under SD conditions. Infrared imaging was used to monitor seedling growth from 2 day onwards every half an hour. Values are the mean of seven seedlings. Error bars indicate SEM. These data are shown in Fig. 2E as growth ratio difference between Col-0 and *toc1*.

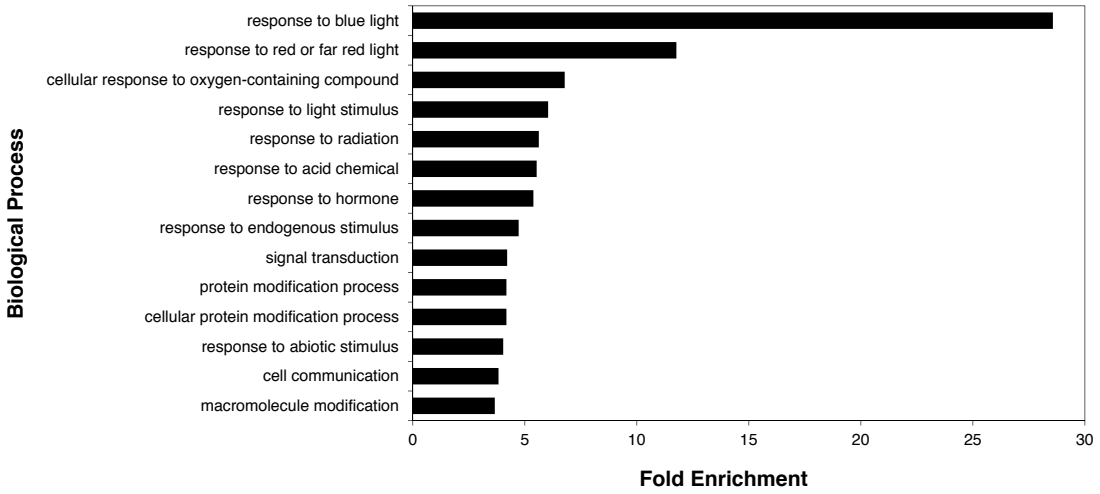

Fig. S10. Functional categorization of the genes in the "dawn-specific PIF-TOC1" gene set. Functional classification of the 49 "dawn-specific PIF-TOC1" genes (defined in Fig. 1B and Supplementary Text) based on Biological Process was done using the gene ontology (GO) enrichment analysis tool (http://geneontology.org/page/go-enrichment-analysis). The figure shows the fold enrichment (count/expected) for the categories identified as significantly overrepresented (pvalue <0.5).

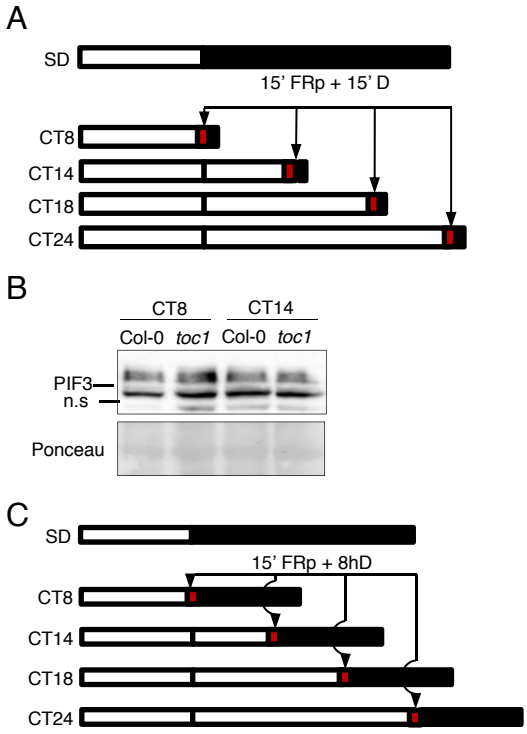

Fig. S11. Analysis of TOC1 gating of shade-stimulated PIF-mediated growth. (A) Diagram of the experimental design used for the gene expression experiment in Fig. 4D and 4E. Seedlings were grown for 2 days in SD conditions and were then released into continuous white light. A 15-min FR pulse (FRp) was given during the third day of growth at the times indicated: CT8, CT14, CT18, and CT24. After the FRp, seedlings were kept in the dark for 15 min. Controls were harvested before the FRp. White, red, and black rectangles represent light, FRp, and darkness, respectively. (B) Immunoblot of endogenous PIF3 in Col-0 wild-type and *toc1* seedlings after the 15-min FRp given at CT8 and CT14 as described in (A). (C) Diagram of the experimental design used for the hypocotyl elongation experiment shown in Fig. 4F. Seedlings were grown for 2 days in SD conditions and were then released into continuous white light. A 15-min FRp was given during the third day of growth at the times indicated: CT8, CT14, CT18, and CT24. After the FRp, seedlings were kept in dark for 8 h. Controls were measured before the FRp. White, red, and black rectangles represent light, FRp, and darkness, respectively.

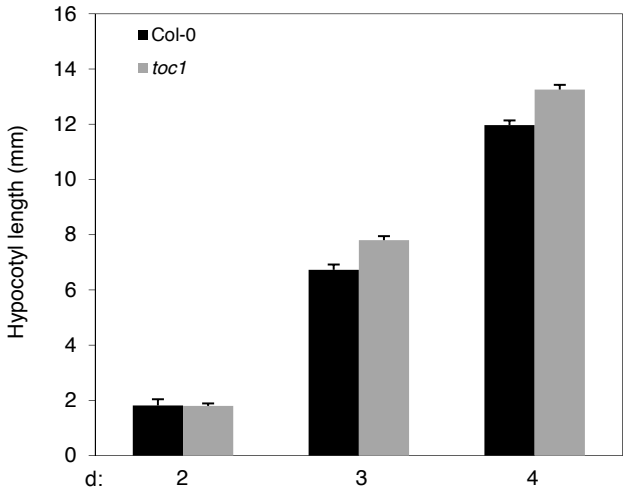

Fig. S12. Involvement of TOC1 in the regulation of hypocotyl elongation during seedling etiolation. Quantification of hypocotyl length in etiolated wild-type Col-0 and *toc1* seedlings. d: days in dark. Error bars indicate SEM.

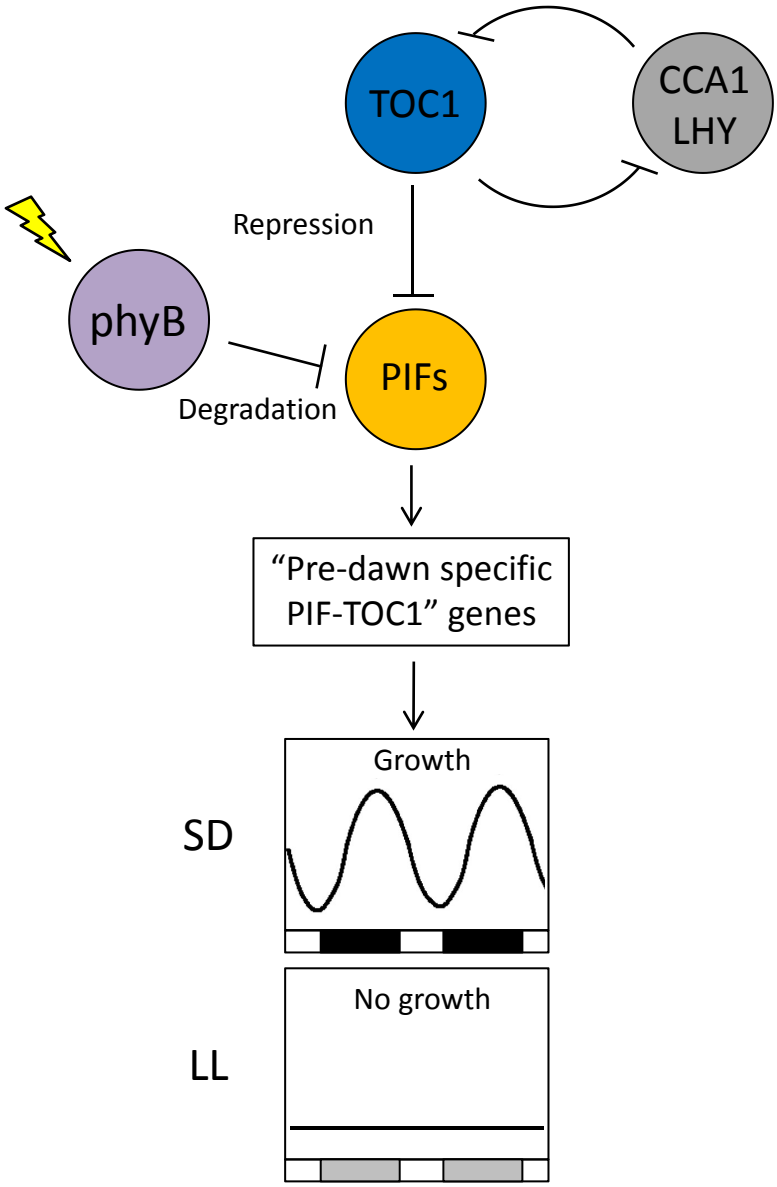

Fig. S13. Phytochrome-photosensory and clock signaling pathways converge directly through shared binding to, and negative regulation of, PIF transcriptional activators. (Top) TOC1 and CCA1/LHY are part of the core clock oscillator in Arabidopsis and inhibit each other's transcription. TOC1 also connects directly to a set of output genes by repressing dark-induced, PIF-activated genes, during the early hours of diurnal darkness, through evening-phased accumulation of TOC1. (Bottom) Under short day conditions (SD), PIF-induced non-core-clock output genes of TOC1 sustain robust oscillations that peak at dawn. However, under free-running conditions of constant light (LL), where PIF levels are low due to phytochrome-mediated degradation, core-clock generated oscillations in TOC1 abundance lose the capacity to generate sustained entrained oscillations in LL (Fig. 3A and S5), because PIF levels are too low to activate those genes.